Effect of Phosphorothioate Chirality on i-Motif Structure and Stability†

Kenji Kanaori,*,‡ Shunji Sakamoto,§ Hiroyuki Yoshida,§ Pitor Guga,|| Wojtech Stec,|| Kunihiko Tajima,‡ and Keisuke Makino⊥

Departments of Applied Biology and of Polymer Science and Engineering, Kyoto Institute of Technology, Matsugasaki, Sakyo-ku, Kyoto 606-8585, Japan, Department of Bioorganic Chemistry, Centre of Molecular and Macromolecular Studies, Polish Academy of Sciences, 90-363 Lodz, Poland, and Institute of Advanced Energy, Kyoto University, Gokasho, Uji 611-0011, Japan

Received August 8, 2003; Revised Manuscript Received October 24, 2003

ABSTRACT: The P-chiral stereo-defined phosphorothioate groups have been introduced into all of the four internucleotide positions of d($T_{PS1}C_{PS2}C_{PS3}C_{PS4}C$) (PS*n* = phosphorothioate group), and among the 16 possible diastereomers of PS-d(TC_4), 10 stereomers have been synthesized to investigate the effects of the sense of the P-chirality upon the structure and stability of the i-motif structure. The temperature dependence of circular dichroism spectra showed that the melting temperature (T_m) of the [*all* R_p]-PS-d(TC_4) i-motifs was 31 °C, identical to that of the parent oligomer, PO-d(TC_4), while that of the [*all* S_p]-PS-d(TC_4) i-motif was largely decreased by 11 °C. Single substitution of R_p with S_p caused a decrease of T_m by 3−4 °C at positions of PS1, PS2, and PS3 and by 1 °C at that of PS4, showing the additive property of the T_m suppression. The comparison of the NOESY spectra between [*all* R_p]-PS-, [*all* S_p]-PS-, and PO-d(TC_4) showed that intraresidual H6−H3′ and H2″−H4′ NOE cross-peaks of the *all* S_p isomer are weaker than those of the *all* R_p isomer and PO-d(TC_4), indicating the change in the C3′-endo conformation and glycosidic bond angle. The structural alternation for the i-motif formed by [*all* S_p]-PS-d(TC_4) is also suggested by the chemical shift differences of C2/C3/C4 H2″and H4′ protons from those of [*all* R_p]-PS-d(TC_4) and PO-d(TC_4). These results suggest that the S_p configuration at phosphorus of the phosphorothioate linkage changes the sugar−phosphorothioate conformation and intermolecular interaction in the narrow groove, leading to the destabilization of the i-motif structure.

C-rich DNA oligomers take a unique four-stranded DNA structure, the so-called i-motif, under a slightly acidic or neutral condition (*1*, *2*). The two parallel-stranded duplexes are associated with forming C·C^+ base pairs (Figure 1), their base pairs are fully intercalated, and the relative orientation of the duplexes is antiparallel. Since the first report, a number of similar oligodeoxycytidine sequences have been shown to form stable i-motif structures, and several X-ray structures have been reported (*3*). Viewed down the helical axis, the i-motif has two large and two narrow grooves. Intimate sugar−sugar contacts exist in the narrow groove between residues belonging to different antiparallel strands, possibly involving the CH···O hydrogen bonds across the narrow grooves (*3*, *4*). Investigations of its biological significance have been encouraged by the demonstration and description of the intramolecular i-motif structure of human telomeric and centromeric sequences (*5*, *6*), by the recent observation of an intercalated RNA structure (*7*), and by the discovery of proteins that associate with DNA sequences carrying cytosine repeats (*8*−*11*). It has been pointed out that the compatibility of the C·C^+ intercalation with the modification of the DNA backbone is favorable for aptamer design (*3*). The modifications of the deoxyribose moieties were examined, such as the introduction of D-arabinose, *O*-methyl-*β*-D-ribose, and D-ribose, to investigate the stabilizing factors of this unique DNA structure (*12*). The stability of the chimeric DNA/RNA and RNA i-motif was also reported in which the steric hindrance between 2′-hydroxyl groups in the narrow groove destabilizes the i-motif structure, and the penalty of adding an RNA residue is equal to or greater than the benefit of the additional forming C·C^+ base pairs (*7*, *13*).

Oligodeoxynucleoside phosphorothioate (PS-oligo)[1] is extensively studied for antisense suppression of protein biosynthesis, for drug target validation, and recently also as antisense therapeutic agents (*14*). Such broad application of PS-oligo is due to their nuclease resistance, relatively easy syntheses, high melting temperature of the duplex with complementary target RNA, and susceptibility by RNase H. Among a number of other successful backbone modifications,

† This work was supported by Grants-in-Aid for Encouragement of Young Scientists from the Japan Society for the Promotion of Science to K.K. (13780465 and 15570098) and by Grants-in-Aid for Scientific Research from the Ministry of Education, Science, Sports, and Culture to K.M. (08458176, 10151219, 10878092, 11101001, and 12480173).

* To whom correspondence should be addressed [telephone, +81-(75)-724-7825; fax, +81-(75)-724-7807; e-mail, kanaori@ipc.kit.ac.jp].

‡ Department of Applied Biology, Kyoto Institute of Technology.

§ Department of Polymer Science and Engineering, Kyoto Institute of Technology.

|| Polish Academy of Sciences.

⊥ Kyoto University.

[1] Abbreviations: PS-oligo, oligodeoxynucleoside phosphorothioate; CD, circular dichroism; 1D, one dimensional; 2D, two dimensional; DQF-COSY, double-quantum-filtered correlated spectroscopy; TOCSY, total correlation spectroscopy; NOESY, nuclear Overhauser enhancement spectroscopy; HMQC, heteronuclear multiple-quantum coherence spectroscopy.

10.1021/bi035419r CCC: $27.50
Published on Web 04/23/2004

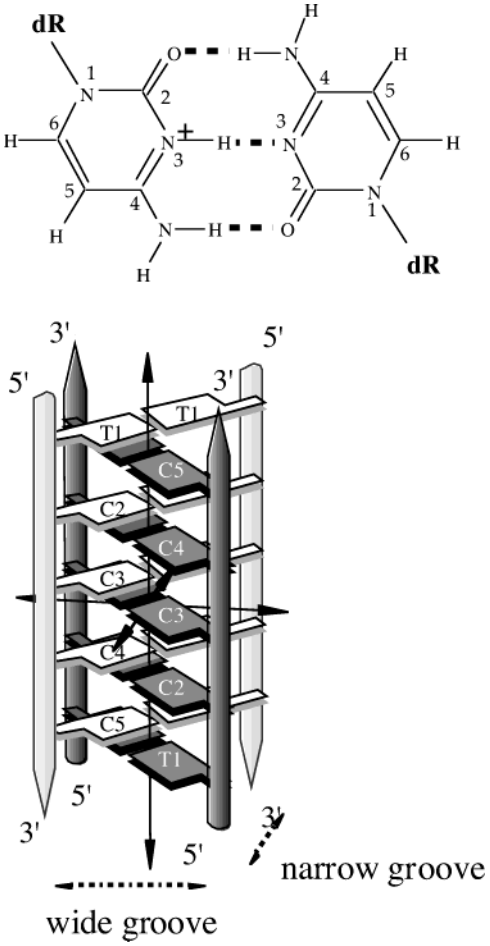

FIGURE 1: Chemical structure of the C·C$^+$ base pair and schematic drawings of the i-motif topology of d(TC$_4$). dR indicates a deoxyribose moiety. The schematic drawing of the i-motif was scanned and modified from the schematic draw of d(TC$_5$) (*2*).

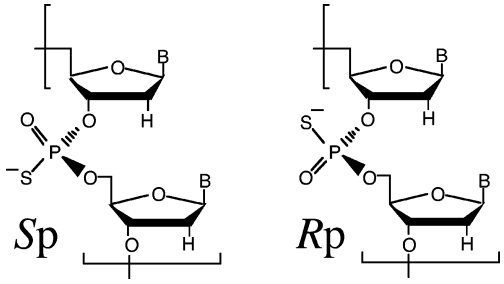

FIGURE 2: Chemical structure of R_p- and S_p-phosphorothioate linkages.

PS-oligo is one of the best backbone modifications to design a DNA aptamer biologically active in vivo, although with some toxicological properties (*15*, *16*). Moreover, oligo(deoxycytidine phosphorothioate)s are interesting in terms of their efficient HIV inhibition and antisense reagent for telomere DNA (*17*, *18*). The P-chirality (S_p and R_p) of the phosphorothioate (Figure 2) is known to change the stability and structure of the PS-oligo duplex with the complementary DNA or RNA (*19*, *20*). We previously reported the i-motif formation of phosphorothioate oligodeoxycytidine [PS-d(C$_n$), $n = 4$, 20], as well as the parent DNA oligomer, and the preliminary study on the effects of the stereo regulation of the phosphorothioate groups on the i-motif stability (*21*). However, the solubility limitation of the PS-d(C$_4$) and its parent oligomers prevented the extensive structural study by NMR spectroscopy, and little is known for the effects of the stereo-defined phosphorothioate on the structure and stability of the i-motif.

Table 1: Melting Temperatures (°C) of i-Motif Structures Formed by PS-d(TC$_4$) Isomers

	configurations[a]						configurations				
no.	PS1	PS2	PS3	PS4	T_m[b]	no.	PS1	PS2	PS3	PS4	T_m
1	*R*	*R*	*R*	*R*	31	**6**	*S*	*S*	*R*	*R*	24
2	*R*	*R*	*S*	*R*	27	**7**	*S*	*R*	*S*	*R*	24
3	*R*	*S*	*R*	*R*	27	**8**	*R*	*S*	*S*	*S*	23
4	*R*	*S*	*R*	*S*	27	**9**	*S*	*S*	*S*	*R*	21
5	*S*	*R*	*R*	*S*	26	**10**	*S*	*S*	*S*	*S*	20

[a] d($T_{PS1}C_{PS2}C_{PS3}C_{PS4}C$) (PS = phosphorothioate group). [b] Standard deviations are ±0.8 °C. T_m penalty values for each phosphorothioate position (PS1−4) are calculated by the following sets of T_m values: PS1, $\Delta T_m^{2-7} = 3$, $\Delta T_m^{3-6} = 3$, and $\Delta T_m^{8-10} = 3$; PS2, $\Delta T_m^{1-3} = 4$ and $\Delta T_m^{7-9} = 3$; PS3, $\Delta T_m^{1-2} = 4$, $\Delta T_m^{3-8} = 4$, and $\Delta T_m^{6-9} = 3$; PS4, $\Delta T_m^{3-4} = 0$ and $\Delta T_m^{9-10} = 1$.

In the present study, we have synthesized 10 diastereomers of phosphorothioate DNA, d($T_{PS1}C_{PS2}C_{PS3}C_{PS4}C$) (PS = phosphorothioate group), by the oxathiaphospholane method (*22*) and systematically investigated positional and consecutive effects of the stereo regulation of the phosphorothioate group on the i-motif stability and structure by circular dichroism (CD) and NMR spectroscopy. The present results provide further detailed information and a prediction about the stability of PS i-motif structures and the origin of the PS-oligo stereo differentiation.

MATERIALS AND METHODS

Sample Preparation. The stereo-defined PS-d(TC$_4$) pentamers (Table 1) were synthesized by the oxathiaphospholane method and purified by reverse-phase HPLC as previously reported (*21*). The CD and NMR samples were prepared in 20 mM acetate buffer (pH 4.5) containing 100 mM NaCl, and their concentrations were estimated using the extinction coefficients at 260 nm which were calculated by the nearest neighbor method. The samples were premelted at 80 °C prior to the measurements to destroy secondary structure and then allowed to thermally equilibrate.

CD Spectroscopy. CD spectra were measured over 200−350 nm on a J-720 spectropolarimeter (Japan Spectroscopic Co.) using a jacketed quartz cell with an optical path length of 0.1 cm. The strand concentration was 100 ± 4.5 μM for all of the samples. The CD cell temperature was regulated by circulating an ethylene glycol/water mixture in the jacket whose temperature was controlled by an RTE-100 thermostat (NESLAB) and monitored by a copper constantan thermocouple (Shimadzu). After each temperature change of about 2 °C, the samples were allowed to stand for 20−40 min for the next measurements until the equilibrium between the monomer and tetrad was reached. Almost identical denaturation curves were obtained by increasing and decreasing temperature for all of the samples, and the standard deviations of the T_m values were ±0.8 °C. The curves were analyzed by a non-least-squares fit method.

NMR Measurements. NMR samples were prepared in 20 mM acetate buffer (pH 4.5) containing 100 mM NaCl. The strand concentration was 3 mM. The sample in an NMR tube was premelted at 80 °C prior to the measurements. Attain-

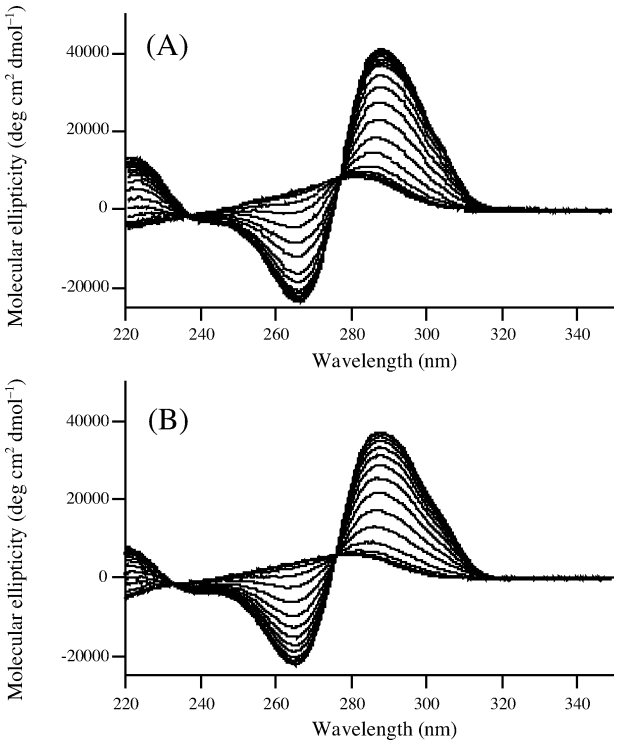

FIGURE 3: Temperature dependence of CD spectra obtained for (A) [*all* R_p]-PS-d(TC_4) and (B) [*all* S_p]-PS-d(TC_4).

ment of the equilibrium among single- and four-stranded components was confirmed by measuring the time course of one-dimensional (1D) ^{1}H NMR spectra. The NMR spectra were recorded on a Bruker ARX-500 spectrometer. For the resonance assignment, two-dimensional (2D) NMR spectra, DQF-COSY (*23*), TOCSY (mixing times 40 and 80 ms) (*24*), NOESY (mixing times 100, 200, and 350 ms) (*25*), and ^{1}H−^{31}P HMQC (*26*) were measured at 20 °C. ^{1}H and ^{31}P chemical shifts were referenced to sodium 3-(trimethylsilyl)propionate-*2,2,3,3-d*$_4$ and 85% H_3PO_4, respectively. The NOESY cross-peak intensities were obtained using the measure-volume tool of FELIX software (Biosym Inc.).

RESULTS

Melting Temperatures of the Stereo-Defined PS i-Motif. The specific Cotton effect appearing in CD spectra of the C-rich DNA oligomer is informative of protonated and nonprotonated cytosine base pairing (*27*, *28*), and an enlarged positive peak at 288 nm and a concomitant negative peak at 265 nm are indicative of the i-motif structure of the C-rich DNA oligomer (*29*). When this structure collapses, this positive peak is lowered with blue shift, and simultaneously the negative peak disappears. Temperature elevation causes unfolding of the i-motif structure of C-rich PO-oligo, although the equilibrium is slowly reached (*30*). Temperature-dependent CD measurements were performed at pH 4.5 for 10 diastereoisomers of PS-d(TC_4) and its parent oligomer, PO-d(TC_4), to compare the thermal stability of the i-motif structure between the P-chiral diastereoisomers. The CD spectral change obtained at 5−50 °C is represented for [*all* R_p]- and [*all* S_p]-PS-d(TC_4) in Figure 3. All of the oligomers showed an identical CD curve which has the positive peak at 288 nm and the negative peak at 265 nm below 10 °C, indicating that all of them take an i-motif structure. Both

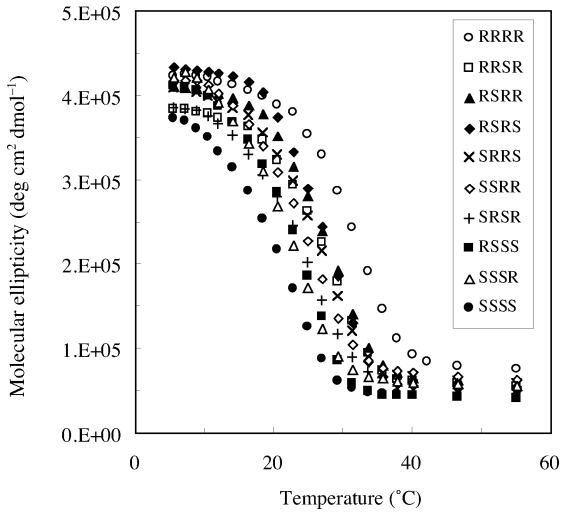

FIGURE 4: Change in the molecular ellipticity at 288 nm as a function of temperature for the 10 PS-d(TC_4) diastereomers.

the positive and negative peaks became smaller with an increase of the temperature. The CD melting profiles were obtained by plotting the molar ellipticity at 288 nm against temperature, as represented in Figure 4. Using this plot, the T_m values were determined for all of the PS-d(TC_4) i-motifs and are summarized in Table 1. The T_m value of the [*all* R_p]-PS-d(TC_4) i-motif was 31 °C, which was identical to that of PO-d(TC_4), while that of the [*all* S_p]-PS-d(TC_4) i-motif was largely decreased by 11 °C. This tendency that the R_p isomer is more stable than the S_p isomer was also confirmed for another sequence of d(C_4T). The T_m values of the [*all* R_p]- and [*all* S_p]-PS-d(C_4T) i-motifs were 25 and <16 °C, respectively. The T_m value of PO-d(C_4T) was 25 °C, identical to that of [*all* R_p]-PS-d(C_4T). These results indicate that T_m differences between *all* R_p and *all* S_p isomers were about 10 °C for four stereo-defined phosphorothioates.

Positional Effect of the Sense of P-Chirality on the Stability of the PS i-Motif. As shown in Table 1, with increase of the number of [S_p]phosphorothioate groups, the T_m values were decreased. To investigate the effect of the P-chirality on the thermal stability of the i-motif in detail, we compared the T_m values of the diastereomeric pairs which differ in a single P-chirality at each internucleotide position. For example, **7**, [S_p,S_p,R_p,R_p]-PS-d(TC_4), is different in the P-chirality at the PS1 position from **2**, [R_p,S_p,R_p,R_p]-PS-d(TC_4), and the T_m value of **7** was lower by 3 °C than that of **2** [$\Delta T_m^{2-7} = T_m$(**2**) − T_m(**7**)]. For the other two pairs, **3**−**6** and **8**−**10**, which differ only in the P-chirality at the position of PS1, ΔT_m^{3-6} and ΔT_m^{8-10} were also 3 °C. Similarly, ΔT_m values for the other three positions were determined to be 3−4 °C at the positions of PS2 and PS3 and ∼1 °C at that of PS4, as shown in Table 1. The T_m values for the PS-d(TC_4) i-motif could be predicted by subtracting the addition of the ΔT_m values from the T_m value of [*all* R_p]-PS-d(TC_4) (31 °C), and the predicted T_m values well coincide with the T_m determined by the denaturation profile. For example, **4**, [R_p,S_p,R_p,S_p]-PS-d(TC_4), has two S_p phosphorothioate linkages at PS2 and PS4, and its T_m value was 27 °C, which is lower by 4 °C than the T_m of [*all* R_p]-PS-d(TC_4). The T_m value of **6**, [S_p,S_p,R_p,R_p]-PS-d(TC_4), was 24 °C, which is lower by 7 °C than that of [*all* R_p]-PS-d(TC_4). These results indicate that the decrease of the T_m values can be predicted by adding

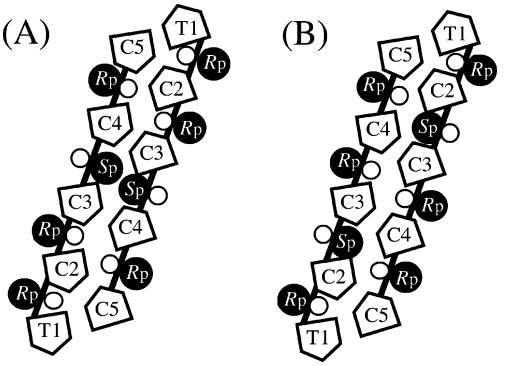

FIGURE 5: Schematic drawing of the two antiparallel strands of the i-motif structure in the narrow groove: (A) [R_p,R_p,S_p,R_p]-PS-d(TC_4) and (B) [R_p,S_p,R_p,R_p]-PS-d(TC_4). A closed and an open circle indicates a sulfur and an oxygen atom of the phosphorothioate group, respectively, and the bases are omitted.

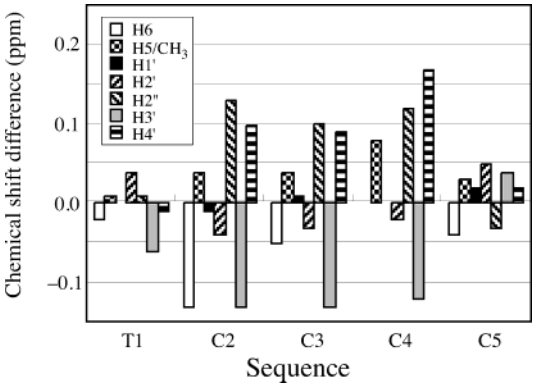

FIGURE 6: ^{1}H chemical shift differences between the stereo-defined PS-d(TC_4) oligomers [δ([*all* S_p]-PS-d(TC_4)) − δ([*all* R_p]-PS-d(TC_4))] for nonlabile protons.

the penalty values at the S_p positions and that the introduction of S_p at the PS4 position has little influence on the stability of the i-motif structure. The almost identical ΔT_m values for the three positions of PS1, PS2, and PS3 indicate that the T_m decrease is independent both of the neighboring P-chirality in the sequence and of the distance between the phosphorothioate groups in the space. For example, on the basis of the i-motif structure of PO-d(TC_5) (*2*), the [S_p]-phosphorothioate groups of **2**, [R_p,R_p,S_p,R_p]-PS-d(TC_4), are located nearby in the narrow groove (Figure 5), where both of the sulfur atoms of the phosphorothioate groups are directed to the inside and the distance between them is about 5 Å. On the other hand, the [S_p]phosphorothioate groups of **3**, [R_p,S_p,R_p,R_p]-PS-d(TC_4), are far apart in the narrow groove (>10 Å). However, these two PS-d(TC_4) showed an identical T_m value as shown in Table 1, indicating that there is no destabilization effect by electric repulsion and steric hindrance between the sulfur atoms of the phosphorothioate groups for the i-motif of **3**. We can conclude that there is no effect of inter- and intramolecular interaction between the phosphorothioate groups on the PS i-motif stability.

Chemical Shift Difference between [all R_p]- and [all S_p]-PS-d(TC_4). To clarify the reason of the T_m decrease by the substitution of R_p with S_p, the structural difference between the i-motifs of [*all* R_p]- and [*all* S_p]-PS-d(TC_4) was investigated by NMR spectroscopy. As a reference molecule, PO-d(TC_4) was also measured in the same conditions as the PS-d(TC_4) i-motifs. The T_m difference of these NMR samples between [*all* R_p]- and [*all* S_p]-PS-d(TC_4) was also determined by integrating the T4 H6 proton signals originating from single- and four-stranded species (*30*). The T_m value of the [*all* R_p]-PS-d(TC_4) i-motif was 46 °C, while that of the [*all* S_p]-PS-d(TC_4) i-motif was 36 °C. The T_m difference was 10 °C, and the tendency that the R_p isomer is more stable than the S_p isomer has been confirmed for the concentrated NMR samples.

Chemical shift change and NOE cross-peak intensities were compared between the i-motifs. To assign the signals of PS-d(TC_4) and PO-d(TC_4), 2D ^{1}H NMR spectra (DQF-COSY, TOCSY, and NOESY) were measured at 20 °C where the proportion of the single-stranded species was not detectable. The assignment was performed analogously to d(TC_n) ($n = 2-5$) on the basis of H1′−H1′ cross-peaks and rectangular pattern of H1′−H6 cross-peaks (*2*, *31*). Those cross-peaks unique for the i-motif were clearly observed for the three PS-d(TC_4) and PO-d(TC_4). The chemical shifts obtained are listed in Table S1. We compared the obtained chemical shift values between PO-d(TC_4), [*all* R_p]-PS-d(TC_4), and [*all* S_p]-PS-d(TC_4). The chemical shift difference ($\Delta\delta$) provides a first approximation of the structure change of the DNA structures, and the differences between [*all* R_p]- and [*all* S_p]-PS-d(TC_4) are shown in Figure 6. The chemical shift differences were also obtained between the PS-d(TC_4) and PO-d(TC_4) i-motifs (Figure S1) to evaluate the direct effect of the substitution of a phosphate with a phosphorothioate group. Remarkable chemical shift changes were observed for H2″, H3′, and H4′ of the central three deoxycytidine residues of C2−C4, while the protons of T1 and C5 were almost identical between [*all* R_p]- and [*all* S_p]-PS-d(TC_4). T1−C4 H3′ protons of both of the PS-d(TC_4) exhibited large downfield shifts from the corresponding protons of the PO-d(TC_4), and the downfield shifts of [*all* R_p]-PS-d(TC_4) were larger than those of [*all* S_p]-PS-d(TC_4) (Figure S1). The same tendency of the chemical shift change of the H3′ proton was previously reported in the NMR study of PS−DNA·DNA and PS−DNA·RNA duplexes containing a stereo-defined phosphorothioate group (*19*). Therefore, the downfield shifts of the H3′ protons are probably attributed not to the structural change but to the induced chemical shift change by the change from a phosphate group to a phosphorothioate group. On the other hand, the C2/C3/C4 H2″ and H4′ protons of [*all* S_p]-PS-d(TC_4) were shifted downfield from the corresponding protons of [*all* R_p]-PS-d(TC_4) and of PO-d(TC_4). Since all three i-motifs showed almost identical shifts for H2′ protons, the periodical differences of the H2″ and H4′ protons may be caused by the structural effects but not by the induced effect. The H2″ and H4′ protons are directed toward the narrow groove of the i-motif, and the intermolecular NOEs of H1′−H2″ and H1′−H4′ between the antiparallel strands indicate that the van der Waals contacts occur at the H1′, H2″, and H4′ part of the deoxyribose moiety (*2*, *31*). These van der Waals contacts are considered to be significant for stabilizing the i-motif structure. The periodical chemical shift differences of the deoxyribose protons suggest that the i-motif structure of [*all* S_p]-PS-d(TC_4) differs in the deoxyribose moieties from [*all* R_p]-PS-d(TC_4) and PO-d(TC_4), although the C·C^+ base stacking is less affected by the introduction of the [S_p]phosphorothioate groups. In addition to the ^{1}H chemical shifts, we examined the ^{31}P

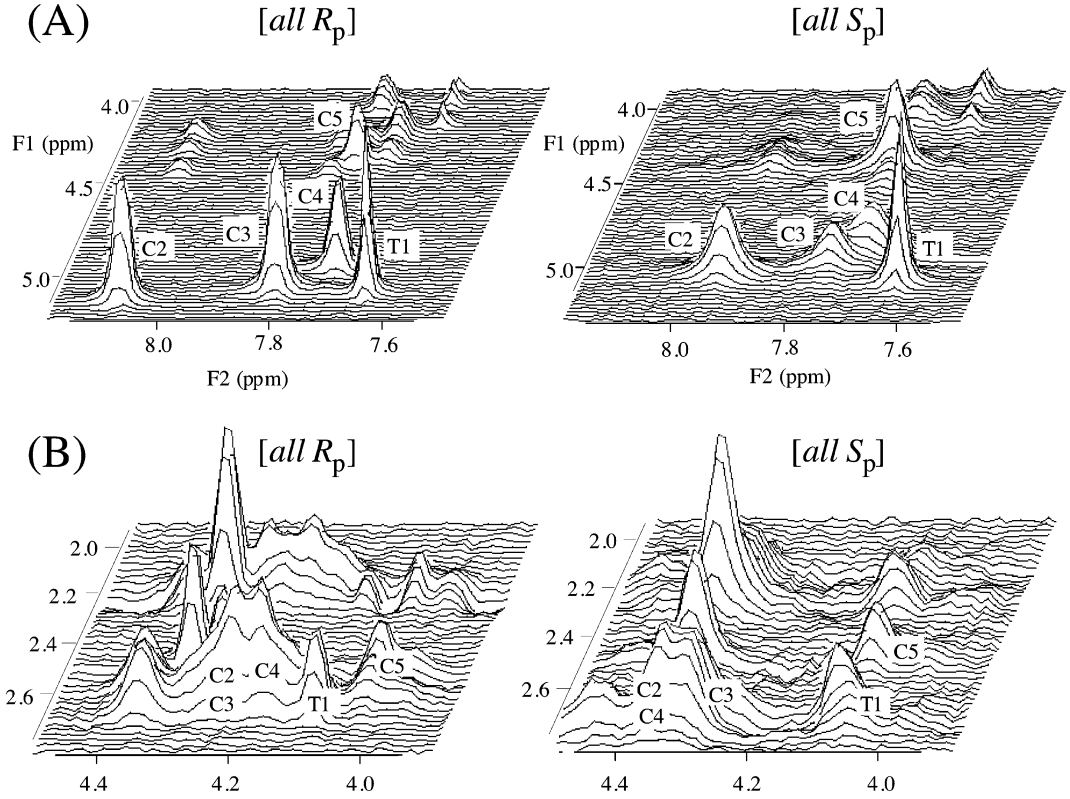

FIGURE 7: 100 ms NOESY spectra for [*all* R_p]- (left) and [*all* S_p]-PS-d(TC_4) (right) measured at 20 °C and pH 4.5. The regions of (A) H3′−H8/H6/H2 and (B) H2′/2″−H4′/H5′/H5″ are displayed with the assignment of intraresidual NOE connectivity indicated by residue names.

chemical shifts of [*all* S_p]-PS-d(TC_4) and [*all* R_p]-PS-d(TC_4) (Table S1). Since the ^{31}P chemical shifts in PS-oligos are different between [R_p]- and [S_p]phosphorothioate (*19*, *32*), we focused on the dispersion of the ^{31}P chemical shifts of the phosphorothioates. As previously reported, ^{31}P NMR signals of the i-motif structure of PO-d(TC_5) were observed in the narrow chemical shift range between −1.0 and 0.5 ppm probably because of its periodical structure (*2*), and ^{31}P chemical shifts of PO-d(TC_4) in this study were also observed in the narrow range between −0.8 and 0.3 ppm. However, the ^{31}P signals of [*all* S_p]-PS-d(TC_4) were observed in the wider range between 55.2 and 57.6 ppm, although those of [*all* R_p]-PS-d(TC_4) were between 55.3 and 56.1 ppm. The dispersion of the ^{31}P chemical shifts of [*all* S_p]-PS-d(TC_4) may be related to the change in the periodical conformation of the phosphorothioate backbone.

Difference in the i-Motif Conformations between [all R_p]- and [all S_p]-PS-d(TC_4). To investigate the i-motif conformations in detail, NOE cross-peak intensities were compared among PO-d(TC_4), [*all* R_p]-PS-d(TC_4), and [*all* S_p]-PS-d(TC_4). There was little difference in intensity of interstrand NOEs of H1′−H1′ and H1′−H6/H6−H1′ between the three oligomers, which is indicative of the i-motif formation. This coincides with the above-mentioned CD results that [*all* S_p]-PS-d(TC_4) takes an i-motif structure although its T_m value is lower than PO-d(TC_4) and [*all* R_p]-PS-d(TC_4). Remarkable differences in the NOE intensities between [*all* R_p]- and [*all* S_p]-PS-d(TC_4) were observed in the H6−H3′ regions of NOESY spectra (Figure 7A). Although the intraresidue H6−H3′ NOE cross-peaks of T1 and C5 were invariant for both of the PS-d(TC_4), those of C2, C3, and C4 of [*all* S_p]-PS-d(TC_4) were weaker than those of [*all* R_p] PS-d(TC_4). The H6−H3′ distances converted from the NOE intensities indicate that those distances of the central deoxycytidine residues of [*all* S_p]-PS-d(TC_4) were longer by 0.2−0.4 Å than those of [*all* R_p]-PS-d(TC_4). The intraresidual H6−H3′ distance generally depends on the pseudorotation phase angle *P* and glycosidic torsion angle χ. Most i-motif structures reported so far take a C3′-endo conformation where the intraresidual H6−H3′ distance is outstandingly short (*2*, *31*). The longer H6−H3′ distances of [*all* S_p]-PS-d(TC_4) may be caused by a conformational change from C3′-endo to C4′-exo and by a decrease in the χ angle. To confirm the conformational change in the deoxyribose moieties, we compared the sum of the couplings, $\sum 1' (= {}^3J_{1',2'} + {}^3J_{1',2''})$, which is related to the geometry of the deoxyribose ring (*33*). The $\sum 1'$ values of T1 and C5 were 12 Hz for both the [*all* R_p]- and [*all* S_p]-PS-d(TC_4), indicating that the *P* values of these terminal residues are about 36°. For the central deoxycytidine residues, $\sum 1'$ values of C2 were 10 Hz (P = 18°) identical for [*all* R_p]- and [*all* S_p]-PS-d(TC_4), while the coupling constants of C3 and C4 could not be determined for both of the PS-d(TC_4) because of signal overlapping. The converted H6−H3′ distances and these coupling constant data indicate that all of the deoxyriboses for both of the PS-d(TC_4) take a conformation in the range between C3′-endo and C4′-exo and that the increase of the H6−H3′ distances of [*all* S_p]-PS-d(TC_4) is caused by the increase in the *P* values of the central deoxycytidine residues, accompanied by a decrease in the χ angles.

The same tendency as observed for the H6−H3′ NOEs was obtained for the NOE intensities in the H2′/H2″−H4′/H5′/H5″ region (Figure 7B): The NOE intensities of [*all* S_p]-PS-d(TC_4) were weaker than those of [*all* R_p]-PS-d(TC_4).

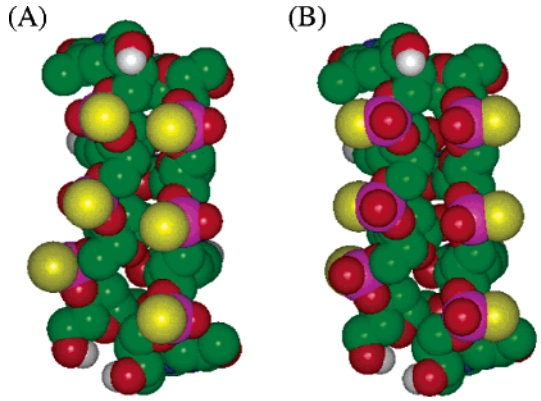

FIGURE 8: View of molecular models of the (A) [*all* S_p]- and (B) [*all* R_p]-PS i-motif in van der Waals space-filling mode viewed from a narrow groove. The coordinates of the i-motif structure are derived from A and D chains of d(C_3T) (PDB code 191D) whose *pro*-S_p or *pro*-R_p oxygen atoms (red) are replaced by a sulfur atom (yellow).

As previously reported, strong NOE cross-peaks are observed in the H2′/H2″−H4′/H5′/H5″ region for the i-motif, because the deoxyriboses of the i-motif structure take C3′-endo where a distance of H2″−H4′ is also very short (<2.5 Å) and because the interresidue NOEs of H2″−H4′ could be observed between the antiparallel strands in the narrow groove (*2*, *31*). Therefore, the weaker NOE peaks in the H2′/H2″−H4′/H5′/H5″ region also indicate that [*all* S_p]-PS-d(TC_4) takes a different deoxyribose conformation in the central C2, C3, and C4 residues, as compared to PO-d(TC_4) and [*all* R_p]-PS-d(TC_4). It was reported that the C3′-endo conformation contributes to the stabilization of the i-motif structure by the intermolecular contacts between the deoxyriboses in the narrow grooves (*2*, *4*, *34*). These results imply that the conformational change (*P* and χ) of the central deoxycytidine residues is induced by the [S_p]phosphorothioate groups, leading to the destabilization of the [*all* S_p]-PS-d(TC_4) i-motif.

DISCUSSION

With the increase in the number of [S_p]phosphorothioate groups, the T_m values of the PS-d(TC_4) i-motifs were decreased. Single replacement of R_p by S_p caused a decrease of T_m by 3−4 °C at positions of PS1, PS2, and PS3 and by 1 °C at that of PS4 with the additive property of the T_m decreases. There was no additional loss in the i-motif stability in terms of the mutual position of the phosphorothioate groups. Such an additive property was also observed for the chimeric DNA/RNA i-motif structure: for each RNA residue added, the T_m decreases by roughly 6.5 °C, while the juxtaposition of the two ribose sugars in a back-to-back orientation incurs an additional loss of 3 °C in the stability (*13*). The ribose 2′-hydroxyl groups are directly involved in the close contacts between the deoxyriboses of the antiparallel strands in the narrow groove and are separated by less than 5 Å in the back-to-back orientation. Therefore, the introduction of the 2′-hydroxyl group makes a larger influence on the i-motif stability and the additional factor for the relative orientation of the riboses. The sulfur atom of the S_p isomer is also directed toward the narrow groove where the deoxyriboses of the antiparallel strands closely contact each other (Figure 8) (*1*, *2*). The destabilization may be caused by the higher steric hindrance and the more negative charge of the sulfur atom as compared with the oxygen atom (*35*). Comparison of NMR spectra between [*all* R_p]- and [*all* S_p]-PS-d(TC_4) indicates the change of the deoxyribose conformation in the center of the i-motif structure (Figure 7). The structure change for the [*all* S_p]-PS-d(TC_4) i-motif is also suggested by the chemical shift change from [*all* S_p] PS-d(TC_4) and PO-d(TC_4) (Figures 6 and S1). These NMR results suggest that this steric hindrance changes the C3′-endo conformation contributing to the stabilization of the i-motif structure by the intermolecular van der Waals contacts between the deoxyriboses in the narrow grooves (*2*, *4*, *34*). Besides the decrease of the van der Waals contacts, the change in the CH···O hydrogen bonds from the O4′ atom may be another possible factor of the destabilization of the [*all* S_p]-PS-d(TC_4) i-motif (*3*, *4*). The inter- and intramolecular CH···O hydrogen bonds possibly play an important role in the intimate sugar−sugar contacts existing in the narrow groove (*3*, *4*). The direction of the lone pair electrons of the O4′ atom is significant in this CH···O hydrogen bond, and the conformational change of the deoxyribose would alter the hydrogen-bonding network in the narrow groove. Thus, the S_p stereo regulation of the phosphorothioate linkage may destabilize the hydrogen bonding through the deoxyribose conformational change. The ΔT_m value for PS4 was much smaller than those for the others. The low penalty value at the PS4 indicates that the deoxyribose moiety of the 3′-terminal residue makes little contribution to the stabilization of the i-motif structure. One reason is that the deoxyribose moiety of the 3′-terminal residue is located outside the stacked C·C^+ planes and may make weak van der Waals contacts in the narrow groove.

Thermodynamic data regarding the influence of P-chirality on stability of duplexes formed between phosphorothioate DNA oligonucleotides and complementary DNA or RNA strands were reported recently (*20*). The relative stability of those duplexes ([*all* R_p]-PS-DNA/DNA vs [*all* S_p]-PS-DNA/DNA) depends on their sequential composition rather than on the absolute configuration of PS-oligos. On the other hand, the [*all* R_p]-PS isomers form more stable duplexes with RNA templates than the [*all* S_p]-PS isomers, which is independent of the sequence. PS−DNA/RNA duplexes take an A-type conformation with a C3′-endo puckering (*19*, *36*, *37*), and the A-type conformation involves sequence-independent water bridges between *pro*-R_p oxygen atoms of adjacent phosphate groups (*38*−*40*). The sequence-independent factor for the stabilization of [*all* R_p]-PS-DNA/RNA is considered to be the hydration effect in the major groove (*20*). The present results show that the T_m decrease is independent both of the neighboring P-chirality in the sequence and of the distance between the phosphorothioate groups in the space. Therefore, such water molecules bridging in the narrow groove would not be related with the stereo differentiation of the stability of the i-motif. In the crystal structure of the d(CCCT) i-motif (PDB code 191D), no significant water molecules were observed between the phosphate groups in the narrow groove (*41*). On the other hand, the crystal structure shows that particular hydration water molecules exist between the *pro*-R_p oxygen atom and cytosine NH_2 of the antiparallel strand in the wide groove. These water molecules may play a similar role in stabilizing the [*all* R_p]-PS i-motif: The sulfur atom in a phosphorothioate group,

carrying most of the negative charge of the internucleotide linkage, is a strong acceptor of the charge-assisted hydrogen bond (*42*). Simultaneously, a nonbridging oxygen in the phosphorothioate group is a much weaker acceptor because of its reduced charge, compared to the symmetrically distributed charge in the unmodified phosphate bond. The hydration pattern in the wide groove can be formed in the case of R_p isomers but not of S_p ones, resulting in the destabilization of the i-motif.

The T_m results in this study are in disagreement with those previously obtained for PS-d(C_4) whose S_p isomer is more stable than R_p (*21*). A possible reason is that the i-motif structure of d(C_4) (NDB code UDD024) is different from all of the other i-motif structures in terms of a small twist angle and C4′-exo deoxyribose conformation (*34*, *43*). As for C−H···O hydrogen networks, the i-motif of d(C_4) has some plasticity in interaction of the O4′ α lone pair with C1′−H1′ and C4′−H4′ (*4*). The structural specificity of the d(C_4) i-motif should cause the opposite effect on the stability of the stereo-defined PS i-motif by the change of the steric hindrance, the C−H···O interaction, or the hydration pattern.

Effects of the phosphorothioate group on the structure and stability have been clarified for various DNA structures. Our observation may become fundamental data for the design of the PS−DNA aptamer using the i-motif structure or other compact DNA structures such as the G-quartet, some of which also show efficient HIV inhibition (*44*, *45*).

SUPPORTING INFORMATION AVAILABLE

^{1}H and ^{31}P NMR assignment of the three i-motifs (Table S1) and chemical shift differences obtained between the PS-d(TC_4) and PO-d(TC_4) i-motifs (Figure S1). This material is available free of charge via the Internet at http://pubs.acs.org.

REFERENCES

1. Leroy, J. L., Gehring, K., Kettani, A., and Guéron, M. (1993) Acid multimers of oligodeoxycytidine strands: stoichiometry, base-pair characterization, and proton exchange properties, *Biochemistry 32*, 6019−6031.
2. Gehring, K., Leroy, J. L., and Guéron, M. (1993) A tetrameric DNA structure with protonated cytosine·cytosine base pairs, *Nature (London) 363*, 561−565.
3. Guéron, M., and Leroy, J.-L. (2000) The i-motif in nucleic acids, *Curr. Opin. Struct. Biol. 10*, 326−331.
4. Berger, I., Egli, M., and Rich, A. (1996) Inter-strand C−H···O hydrogen bonds stabilizing four-stranded intercalated molecules: stereoelectronic effects of O4′ in cytosine-rich DNA, *Proc. Natl. Acad. Sci. U.S.A. 93*, 12116−12121.
5. Gallego, J., Chou, S.-H., and Reid, B. R. (1997) Centromeric pyrimidine strands fold into an intercalated motif by forming a double hairpin with a novel T:G:G:T tetrad: Solution structure of the d(TCCCGTTTCCA) dimer, *J. Mol. Biol. 273*, 840−856.
6. Phan, A. T., Guéron, M., and Leroy, J. L. (2000) The solution structure and internal motions of a fragment of the cytidine-rich strand of the human telomere, *J. Mol. Biol. 299*, 123−144.
7. Snoussi, K., Nonin, S.-L., and Leroy, J. L. (2001) The RNA i-motif, *J. Mol. Biol. 309*, 139−153.
8. Marsich, E., Xodo, L. E., and Manzini, G. (1998) Widespread presence in mammals and high binding specificity of a nuclear protein that recognises the single-stranded telomeric motif $(CCCTAA)_n$, *Eur. J. Biochem. 258*, 93−99.
9. Marsich, E., Piccini, A., Xodo, L. E., and Manzini, G. (1996) Evidence for a HeLa nuclear protein that binds specifically to the single-stranded d$(CCCTAA)_n$ telomeric motif, *Nucleic Acids Res. 24*, 4029−4033.
10. Lacroix, L., Lienard, H., Labourier, E., Djavaheri-Mergny, M., Lacoste, J., Leffers, H., Tazi, J., Helene, C., and Mergny, J.-L. (2000) Identification of two human nuclear proteins that recognise the cytosine-rich strand of human telomeres in vitro, *Nucleic Acids Res. 28*, 1564−1575.
11. Cornuel, J. F., Moraillon, A., and Guéron, M. (2002) Participation of yeast inosine 5′-monophosphate dehydrogenase in an in vitro complex with a fragment of the C-rich telomeric strand, *Biochimie 84*, 279−289.
12. Robidoux, S., and Damha, M. J. (1997) D-2′-Deoxyribose and D-arabinose, but not D-ribose, stabilize the cytosine tetrad (i-DNA) structure, *J. Biomol. Struct. Dyn. 15*, 529−535.
13. Collin, D., and Gehring, K. (1998) Stability of chimeric DNA/RNA cytosine tetrads: Implications for i-motif formation by RNA, *J. Am. Chem. Soc. 120*, 4069−4072.
14. Agrawal, S., and Kandimalla, E. R. (2000) Antisense therapeutics: Is it as simple as complementary base recognition?, *Mol. Med. Today 6*, 72−81.
15. Crooke, S. T. (1995) *Therapeutic applications of oligonucleotides*, R. G. Landes Co., Georgetown, TX.
16. Zon, G., and Stec, W. J. (1991) in *Oligonucleotides and analogues: A practical approach* (Eckstein, F., Ed.), IRL Press, London.
17. Matsukura, M., Zon, G., Shinozuka, K., Stein, C. A., Mitsuya, H., Cohen, J. S., and Broder, S. (1988) Synthesis of phosphorothioate analogues of oligodeoxyribonucleotides and their antiviral activity against human immunodeficiency virus (HIV), *Gene 72*, 343−347.
18. Matsukura, M., Shinozuka, K., Zon, G., Mitsuya, H., Reitz, M., Cohen, J. S., and Broder, S. (1987) Phosphorothioate analogs of oligodeoxynucleotides: Inhibitors of replication and cytopathic effects of human immunodeficiency virus, *Proc. Natl. Acad. Sci. U.S.A. 84*, 7706−7710.
19. Kanaori, K., Tamura, Y., Wada, T., Nishi, M., Kanehara, H., Morii, T., Tajima, K., and Makino, K. (1999) Structure and stability of the consecutive stereoregulated chiral phosphorothioate DNA duplex, *Biochemistry 38*, 16058−16066.
20. Boczkowska, M., Guga, P., and Stec, W. J. (2002) Stereodefined phosphorothioate analogues of DNA: relative thermodynamic stability of the model PS-DNA/DNA and PS-DNA/RNA complexes, *Biochemistry 41*, 12483−12487.
21. Kanehara, H., Mizuguchi, M., Tajima, K., Kanaori, K., and Makino, K. (1997) Spectroscopic evidence for the formation of four-stranded solution structure of oligodeoxycytidine phosphorothioate, *Biochemistry 36*, 1790−1797.
22. Stec, W. J., Karwowski, B., Boczkowska, M., Guga, P., Koziolkiewicz, M., Sochacki, M., Wieczorek, M. W., and Blaszczyk, J. (1998) Deoxyribonucleoside 3′-O-(2-thio- and 3′-O-(2-oxo-"spiro"-4.4-pentamethylene-1.3.2-oxathiaphospholanes): Monomers for stereocontrolled synthesis of oligo(nucleoside phosphorothioate)s and chimeric PS/PO oligonucleotides, *J. Am. Chem. Soc. 120*, 7156−7167.
23. Piantini, U., Sørensen, O. W., and Ernst, R. R. (1982) Multiple quantum filters for elucidating NMR coupling networks, *J. Am. Chem. Soc. 104*, 6800−6801.
24. Davis, D. G., and Bax, A. (1985) Assignment of complex proton NMR spectra via two-dimensional homonuclear Hartmann−Hahn spectroscopy, *J. Am. Chem. Soc. 107*, 2820−2821.
25. Jeener, J., Meier, B. H., Bachmann, P., and Ernst, R. R. (1979) Investigation of exchange processes by two-dimensional NMR spectroscopy, *J. Chem. Phys. 71*, 4546−4553.
26. Blommers, M. J. J., van de Ven, F. J. M., van der Marel, G. A., van Boom, J. H., and Hilbers, C. W. (1991) The three-dimensional structure of a DNA hairpin in solution two-dimensional NMR studies and structural analysis of d(ATCCTATTTATAGGAT), *Eur. J. Biochem. 201*, 33−51.
27. Edwards, E. L., Ratliff, R. L., and Gray, D. M. (1988) Circular dichroism spectra of DNA oligomers show that short interior stretches of C·C^+ base pairs do not form in duplexes with A.T base pairs, *Biochemistry 27*, 5166−5174.
28. Edwards, E. L., Patrick, M. H., Ratliff, R. L., and Gray, D. M. (1990) A·T and C·C^+ base pairs can form simultaneously in a novel multistranded DNA complex, *Biochemistry 29*, 828−836.
29. Manzini, G., Yathindra, N., and Xodo, L. E. (1994) Evidence for intramolecularly folded i-DNA structures in biologically relevant CCC-repeat sequences, *Nucleic Acids Res. 22*, 4634−4640.
30. Kanaori, K., Maeda, A., Kanehara, H., Tajima, K., and Makino, K. (1998) ^{1}H nuclear magnetic resonance study on equilibrium between two four-stranded solution conformations of short d(C_nT), *Biochemistry 37*, 12979−12986.

31. Leroy, J. L., and Guéron, M. (1995) Solution structures of the i-motif tetramers of d(TCC), d(5methylCCT) and d(T5methylCC): novel NOE connections between amino protons and sugar protons, *Structure 3*, 101−120.
32. Stec, W. J., Grajkowski, A., Kobylanska, A., Karwowski, B., Koziolkiewicz, M., Misiura, K., Okruszek, A., Wilk, A., Guga, P., and Boczkwaska, M. (1995) Diastereomers of nucleoside 3′-O-(2-thio-1,3,2-oxathia(selena)phospholanes): Building blocks for sterecontrolled synthesis of oligo(nucleoside phosphorothioate)s, *J. Am. Chem. Soc. 117*, 12019−12029.
33. Rinkel, L. J., and Altona, C. (1987) Conformational analysis of the deoxyribofuranose ring in DNA by means of sums of proton−proton coupling constants: a graphical method, *J. Biomol. Struct. Dyn. 4*, 621−649.
34. Berger, I., Cai, L., Chen, L., and Rich, A. (1997) Energetics of the lattice: packing elements in crystals of four-stranded intercalated cytosine-rich DNA molecules, *Biopolymers 44*, 257−267.
35. Frey, P. A., and Sammons, R. D. (1985) Bond order and charge localization in nucleoside phosphorothioates, *Science 228*, 541−545.
36. González, C., Stec, W., Kobylanska, A., Hogrefe, R. I., Reynolds, M., and James, T. L. (1994) Structural study of a DNA·RNA hybrid duplex with a chiral phosphorothioate moiety by NMR: extraction of distance and torsion angle constraints and imino proton exchange rates, *Biochemistry 33*, 11062−11072.
37. Furrer, P., Billeci, T. M., Donati, A., Kojima, C., Karwowski, B., Sierzchala, A., Stec, W., and James, T. L. (1999) Structural effect of complete [Rp]-phosphorothioate and phosphorodithioate substitutions in the DNA strand of a model antisense inhibitor-target RNA complex, *J. Mol. Biol. 285*, 1609−1622.
38. Egli, M., Tereshko, V., Teplova, M., Minasov, G., Joachimiak, A., Sanishvili, R., Weeks, C., Miller, R., Maier, M., An, H., Dan Cook, P., and Manoharan, M. (1998) X-ray crystallographic analysis of the hydration of A- and B-form DNA at atomic resolution, *Biopolymers 48*, 234−252.
39. Sundaralingam, M., and Pan, B. (2002) Hydrogen and hydration of DNA and RNA oligonucleotides, *Biophys. Chem. 95*, 273−282.
40. Auffinger, P., and Westhof, E. (2001) RNA solvation: a molecular dynamics simulation perspective, *Biopolymers 56*, 266−274.
41. Kang, C. H., Berger, I., Lockshin, C., Ratliff, R., Moyzis, R., and Rich, A. (1994) Crystal structure of intercalated four-stranded d(C_3T) at 1.4 Å resolution, *Proc. Natl. Acad. Sci. U.S.A. 91*, 11636−11640.
42. Boczkowska, M., Guga, P., Karwowski, B., and Maciaszek, A. (2000) Effect of P-chirality of internucleotide bonds on B−Z conversion of stereodefined self-complementary phosphorothioate oligonucleotides of the [PS]-d(CG)$_4$ and [PS]-d(GC)$_4$ series, *Biochemistry 39*, 11057−11064.
43. Chen, L., Cai, L., Zhang, X., and Rich, A. (1994) Crystal structure of a four-stranded intercalated DNA: d(C_4), *Biochemistry 33*, 13540−13546.
44. Jing, N., and Hogan, M. E. (1998) Structure−activity of tetrad-forming oligonucleotides as a potent anti-HIV therapeutic drug, *J. Biol. Chem. 273*, 34992−34999.
45. Rando, R., Ojwang, J., Elbaggari, A., Reyes, G., Tinder, R., McGrath, M., and Hogan, M. (1995) Suppression of human immunodeficiency virus type 1 activity in vitro by oligonucleotides which form intramolecular tetrads, *J. Biol. Chem. 270*, 1754−1760.

BI035419R